Decanuclear Manganese(III) Complexes with the $[Mn_{10}O_8]^{14+}$ Core: Structural and Magnetochemical Characterization of $[Mn_{10}O_8(O_2CPh)_6(chel)_8]$ (chel = pic, dbm)

Hilary J. Eppley,[1a] Sheila M. J. Aubin,[1b] William E. Streib,[1a] John C. Bollinger,[1a] David N. Hendrickson,*[,1b] and George Christou*[,1a]

Department of Chemistry and the Molecular Structure Center, Indiana University, Bloomington, Indiana 47405-4001, and the Department of Chemistry−0358, University of California at San Diego, La Jolla, California 92093-0358

Received June 26, 1996[⊗]

The preparation and properties are described of two related Mn_{10} clusters with the same $[Mn_{10}O_8]^{14+}$ (10 Mn^{III}) core. Dissolution of $[Mn_4O_2(O_2CPh)_6(MeCN)_2(pic)_2]$ (**1**) in $MeCONMe_2$ (DMA) and CH_2Cl_2 in the presence of picH (picolinic acid) leads to slow crystallization of $[Mn_{10}O_8(O_2CPh)_6(pic)_8]$ (**2**) in 50−55% yield. The same reaction in the presence of dibenzoylmethane (dbmH) instead of picH gives $[Mn_{10}O_8(O_2CPh)_6(pic)_6(dbm)_2]$ (**3**). Complex **2**·$6CH_2Cl_2$ crystallizes in the monoclinic space group $P2_1/n$ with (at −169 °C) a = 14.987(3) Å, b = 17.177(3) Å, c = 21.250(4) Å, β = 91.48(1)°, and Z = 2. Complex **3**·$3CH_2Cl_2$ crystallizes in the triclinic space group $P\bar{1}$ with (at −165 °C) a = 14.892(6) Å, b = 15.537(6) Å, c = 14.697(6) Å, α = 109.82(2)°, β = 97.75-(2)°, γ = 111.66(2)°, and Z = 1. The two structures are very similar, differing only in the chelate identity at two positions, and resulting small perturbations in some metric parameters. Variable-temperature magnetic susceptibility data were obtained for **2**·$3H_2O$ with a dc SQUID in the range 2.00−320 K and in a 10 kG applied field. The effective magnetic moment (μ_{eff}) per molecule slowly decreases from 14.28 μ_B at 320 K to 4.94 μ_B at 2.00 K. Data were also collected with an ac SQUID in the range 2.00−30.0 K in a 1 G field oscillating at 250 Hz. The ac data essentially superimpose on the dc data except at temperatures ≤6 K. The combined results indicate a S_T = 0 ground state for **2** with a very low-lying excited state(s) that is (are) populated even at 2.00 K. The possibility of a S_T = 1 (or even S_T = 2) ground state cannot be completely ruled out, however, in the absence of data at <2 K.

Introduction

Manganese carboxylate chemistry continues to be a rich source of cluster complexes with a variety of metal nuclearities, currently up to 18,[2−10] and at a range of oxidation levels spanning individual metal oxidation states of II−IV. Our interest in this area has been stimulated by a number of factors, including the aesthetically pleasing structures of Mn carboxylate clusters and their propensity to exhibit highly unusual magnetic properties. Thus, (i) they often display high spin (S) values[3a,5b,8] in the ground state, a property resulting from the presence of at least some intramolecular exchange interactions that are ferromagnetic in nature and/or the presence of spin frustration effects; and (ii) certain complexes have been identified as being able to be magnetized below a critical temperature owing to certain properties of individual molecules, i.e., they are "single-molecule magnets".[6b,8]

As part of a continuing interest in the structural and magnetic properties of Mn carboxylate clusters, we have been seeking to develop synthetic routes to new examples of such species. Aggregation of preformed, small nuclearity species with $[Mn_3O]^{6+,7+}$ or $[Mn_4O_2]^{8+}$ cores is one method that has proven useful in the past.[2b,3,4a,6,10,11] For example, reaction of $[Mn_4O_2(O_2CMe)_6(py)_2(dbm)_2]$ (dbm^- is the anion of dibenzoylmethane) with Cl^- in CH_2Cl_2 gives the heptanuclear complex $[Mn_7O_4(O_2CMe)_{10}(dbm)_4]^-$ ($7Mn^{III}$),[2b] and reaction of $[Mn_4O_2(O_2CPh)_9(H_2O)]^-$ with Me_3SiCl gives the octanuclear complex $[Mn_8O_6Cl_6(O_2CPh)_7(H_2O)_2]^-$ ($8Mn^{III}$).[3b] Similarly, treatment of $[Mn_4O_2(O_2CPh)_9(H_2O)]^-$ with KHphth ($Hphth^-$ is mon-

[⊗] Abstract published in *Advance ACS Abstracts,* December 1, 1996.

(1) (a) Department of Chemistry and the Molecular Structure Center, Indiana University. (b) University of California at San Diego.
(2) (a) Bhula, R.; Weatherburn, D. C. *Angew. Chem., Int. Ed. Engl.* **1991**, *30*, 688. (b) Wang, S.; Tsai, H.-L.; Streib, W. E.; Christou, G.; Hendrickson, D. N. *J. Chem. Soc., Chem. Commun.* **1992**, 677. (c) Bolcar, M.; Christou, G. Unpublished results.
(3) (a) Wang, S.; Huffman, J. C.; Folting, K.; Streib, W. E.; Lobkovsky, E. B.; Christou, G. *Angew. Chem., Int. Ed. Engl.* **1991**, *30*, 1672. (b) Tsai, H.-L.; Wang, S.; Folting, K.; Streib, W. E.; Hendrickson, D. N.; Christou, G. *J. Am. Chem. Soc.* **1995**, *117*, 2503. (c) Libby, E.; Folting, K.; Huffman, J. C.; Christou, G. *J. Am. Chem. Soc.* **1990**, *112*, 5354. (d) Libby, E.; Folting, K.; Huffman, C. J.; Huffman, J. C.; Christou, G. *Inorg. Chem.* **1993**, *32*, 2549. (e) Wemple, M. W.; Tsai, H.-L.; Streib, W. E.; Hendrickson, D. N.; Christou, G. *J. Chem. Soc., Chem. Commun.* **1994**, 1031.
(4) (a) Christmas, C.; Vincent, J. B.; Chang, H.-R.; Huffman, J. C.; Christou, G.; Hendrickson, D. N. *J. Am. Chem. Soc.* **1991**, *30*, 1672. (b) Low, D. W.; Eichorn, D. M.; Draganescu, A.; Armstrong, W. H. *Inorg. Chem.* **1991**, *30*, 878.
(5) (a) Hagen, K. S.; Armstrong, W. H.; Olmstead, M. M. *J. Am. Chem. Soc.* **1989**, *111*, 774. (b) Goldberg, D. P.; Caneschi, A.; Lippard, S. J. *J. Am. Chem. Soc.* **1993**, *115*, 9299. (c) Goldberg, D. P.; Caneschi, A.; Lippard, S. J. *J. Am. Chem. Soc.* **1995**, *117*, 5789. (d) Cavaluzzo, M.; Chen, Q.; Zubieta, J. *J. Chem. Soc., Chem. Commun.* **1993**, 131. (e) Kolack, K. Unpublished results. (f) Bolcar, M. Unpublished results.
(6) (a) Perlepes, S. P.; Huffman, J. C.; Christou, G. *J. Chem. Soc., Chem. Commun.* **1992**, 1657. (b) Tang, X.; Grillo, V. A. Unpublished results.
(7) Schake, A. R.; Tsai, H.-L.; de Vries, N.; Webb, R. J.; Folting, K.; Hendrickson, D. N.; Christou, G. *J. Chem. Soc., Chem. Commun.* **1992**, 181.
(8) (a) Lis, T. *Acta Crystallogr.* **1980**, *B36*, 2042. (b) Luneau, D.; Savariault, J.-M.; Tuchagues, J.-P. *Inorg. Chem.* **1988**, *27*, 3912. (c) Caneschi, A.; Gatteschi, D.; Sessoli, R.; Barra, A. L.; Brunel, L. C.; Guiolot, M. *J. Am. Chem. Soc.* **1991**, *113*, 5873. (d) Tsai, H.-L.; Hendrickson, D. N.; Eppley, H. J.; de Vries, N.; Folting, K.; Christou, G. *J. Chem. Soc., Chem. Commun.* **1994**, 1745. (e) Eppley, H. J.; Tsai, H.-L.; de Vries, N.; Folting, K.; Christou, G.; Hendrickson, D. N. *J. Am. Chem. Soc.* **1995**, *117*, 301.
(9) Gorun, S. M.; Stibrany, R. T. U.S. Patent 5 041 575, 1991.
(10) (a) Squire, R. C.; Aubin, S. M. J.; Christou, G.; Hendrickson, D. N. *Angew. Chem., Int. Ed. Engl.* **1995**, *34*, 887. (b) Squire, R. C.; Aubin, S. M. J.; Folting, K.; Streib, W. E.; Christou, G.; Hendrickson, D. N. *Inorg. Chem.* **1995**, 6463. (c) Eppley, H.; Christou, G. Unpublished results.
(11) Christou, G. *Acc. Chem. Res.* **1989**, *22*, 328 and references therein.

S0020-1669(96)00754-9 CCC: $14.00

odeprotonated phthalic acid) gives $K_4Mn_{18}O_{16}(O_2CPh)_{22}(phth)_2(H_2O)_4$ ($18Mn^{III}$).[10a,b] We herein describe another use of such an aggregation procedure triggered by solvent to access two decanuclear complexes with a $[Mn_{10}O_8]^{14+}$ core not previously observed, together with the results of variable-temperature magnetic susceptibility studies on one of the complexes to determine the ground state spin value.

Experimental Section

All manipulations were performed under aerobic conditions using materials as received. $(NBu^n_4)[Mn_4O_2(O_2CPh)_7(pic)_2]$[12] (picH = picolinic acid), $[Mn_4O_3Cl_4(O_2CMe)_3(py)_3]$,[13] $[Mn_3O(O_2CMe)_6(py)_3](py)$,[14] and $[Mn_4O_2(O_2CPh)_6(MeCN)_2(pic)_2]$[3d] (**1**) were prepared as described previously (dbmH = dibenzoylmethane, DMA = *N*,*N*-dimethylacetamide).

$[Mn_{10}O_8(O_2CPh)_6(pic)_8]$ (2). Method A. Complex **1** (1.0 g, 0.76 mmol) was dissolved in DMA (5 mL). The solution was filtered, the filtrate was diluted with CH_2Cl_2 (100 mL), and the solution was left undisturbed at room temperature. Large, black, cube-shaped crystals formed slowly over a period of 7 days; a sample kept in contact with the mother liquor provided a suitable crystal for crystallographic studies and was characterized as **2**·$6CH_2Cl_2$. The crystals were collected by filtration, washed with CH_2Cl_2 (2 × 20 mL) and Et_2O (2 × 20 mL), and dried *in vacuo* overnight. The yield was typically ∼15% based on Mn. Dried solid was hygroscopic and analyzed as **2**·$3H_2O$. Anal. Calcd (found) for $C_{90}H_{68}N_8O_{39}Mn_{10}$: C, 44.4 (44.6); H, 2.8 (3.0); N, 4.6 (4.7); Mn, 22.6 (21.5). Selected IR data (KBr disk, cm^{-1}): 1689 (vs), 1608 (w), 1593 (m), 1535 (l), 1491 (w), 1477 (w), 1385 (vs), 1323 (s), 1292 (s), 1257 (m), 1151 (m), 717 (s), 688 (s), 657 (m, br), 617 (m), 576 (m), 465 (m), 426 (w).

Method B. Complex **1** (1.00 g, 0.76 mmol) and picolinic acid (0.113 g, 0.92 mmol) were dissolved with stirring in DMA (6 mL), and the solution was filtered after 15 min to remove a small amount of greenish-brown solid. The filtrate was diluted with CH_2Cl_2 (125 mL), and the solution was left undisturbed at room temperature. After 2 weeks, large black cubes were collected by filtration, washed with CH_2Cl_2 (2 × 10 mL) and Et_2O (2 × 10 mL), and dried in air. The yield was typically 50−55% based on Mn. The IR spectrum was identical to that for material prepared by method A.

$[Mn_{10}O_8(O_2CPh)_6(pic)_6(dbm)_2]$ (3). Complex **1** (1.50 g, 1.15 mmol) and dbmH (0.258 g, 1.15 mmol) were dissolved with stirring in DMA (8 mL). After 15 min, the solution was filtered and the filtrate diluted with CH_2Cl_2 (60 mL). The resulting solution was left undisturbed for 2 weeks, during which time black, cube-shaped crystals formed (the X-ray sample was taken from crystals kept in contact with mother liquor). These were collected by filtration, washed with Et_2O/CH_2Cl_2 (1:1, 3 × 10 mL), and dried *in vacuo*. The yield was typically ∼25% based on Mn. Anal. Calcd (found) for $C_{109}H_{82}N_6O_{38}Cl_2Mn_{10}$ (**3**·CH_2Cl_2·$2H_2O$): C, 48.4 (48.0); H, 3.1 (2.6); N, 3.1 (3.5); Mn, 20.3 (20.8). Selected IR data (KBr, cm^{-1}): 1686 (s), 1591 (m), 1526 (s), 1479 (m), 1391 (s), 1323 (m), 718 (m), 689 (m), 657 (m), 642 (m), 462 (w), 428 (w).

$[Mn_{10}O_8(O_2CMe)_6(pic)_8]$ (4). Method A. $Mn_4O_3Cl_4(O_2CMe)_3(py)_3$ (2.25 g, 2.73 mmol) in CH_2Cl_2 (25 mL) was treated with picH (0.90 g, 7.5 mmol) and NEt_3 (0.80 g, 7.5 mmol), and the solution was stirred for 30 min to give a dark brown solution. This was filtered, and the filtrate was evaporated to dryness under vacuum. The residue was washed with Et_2O/MeCN (5:1, 2 × 30 mL) and redissolved in CH_2Cl_2 (40 mL). After several hours, a microcrystalline precipitate had formed, and this was collected by filtration, washed with CH_2Cl_2 (5 × 5 mL), and dried in air. The yield was ∼20% based on Mn. Anal. Calcd (found) for $C_{60}H_{56}N_8O_{39}Mn_{10}$ (**4**·$3H_2O$): C, 34.9 (35.0); H, 2.7 (3.0); N, 5.4 (5.1); Mn, 26.6 (26.8). Selected IR data (KBr, cm^{-1}): 1688 (s), 1611 (m), 1539 (m), 1404 (m), 1327 (s), 1294 (s), 1260 (m), 1242 (m), 1154 (m), 766 (m), 718 (s), 691 (s), 658 (m), 644 (m), 467 (m).

Method B. $[Mn_3O(O_2CMe)_6(py)_3](py)$ (0.25 g, 0.29 mmol) and picH (0.09 g, 0.73 mmol) were dissolved with stirring in MeCN (25 mL). Solid $NBu^n_4MnO_4$ (0.026 g, 0.072 mmol) was then added in small portions, resulting in a slight darkening of the brown solution. Three drops of H_2O were added, and the solution was then left undisturbed for 1 week. The resulting brown microcrystalline solid was collected by filtration, washed with MeCN (2 × 20 mL), and dried *in vacuo*. The yield was 58% based on Mn. The IR spectrum was identical to that for material from method A.

X-ray Crystallography and Structure Solution. Data were collected for complexes **2**·$6CH_2Cl_2$ ($+h, +k, \pm l$; $6° \le 2\theta \le 45°$) and **3**·$3CH_2Cl_2$ ($+h, \pm k, \pm l$; $6° \le 2\theta \le 45°$) on a Picker four-circle diffractometer; details of the diffractometry, low-temperature facilities, and computational procedures employed by the Molecular Structure Center are available elsewhere.[15] Suitable single crystals were affixed to glass fibers using silicone grease and transferred to the goniostat where they were cooled for characterization and data collection. The structures were solved by direct methods, using MULTAN (**2**) or SHELXTL (**3**), and standard Fourier techniques and refined by full-matrix least-squares.

For **2**·$6CH_2Cl_2$, a systematic search of a limited hemisphere of reciprocal space revealed a primitive monoclinic cell. Following complete data collection, the conditions $h + l = 2n$ for $h0l$ and $k = 2n$ for $0k0$ uniquely determined the space group as $P2_1/n$. Data processing produced a unique set of 7177 intensities and gave a residual of 0.042 for the averaging of 1769 of these which had been measured more than once. Four standards measured every 400 data points showed no significant trends. No correction was made for absorption. The positions of the five manganese atoms in the asymmetric unit were obtained from an initial *E*-map. The positions of the remaining non-hydrogen atoms were obtained from subsequent iterations of least-squares refinement and difference Fourier map calculation. In addition to the atoms of interest, the asymmetric unit contains three molecules of CH_2Cl_2 that had been used as the solvent. The occupancy of the solvent molecules refined to an average of 89%, which was then fixed. One of the chlorine atoms in one of the solvent molecules appeared to be disordered and was refined as atoms Cl(81) and Cl(82) in a 2:1 ratio. Hydrogen atoms were included in fixed calculated positions with thermal parameters fixed at one plus the isotropic thermal parameter of the atom to which they were bonded. In the final cycles of refinement on *F*, the non-hydrogen atoms were varied with anisotropic thermal parameters to give a final $R(F) = 0.058$ for the 740 total variables using all of the unique data; data having $F < 3.0\sigma(F)$ were given zero weight. The final difference Fourier map was essentially featureless, the largest peak being 0.75 and the deepest hole being −0.74 e/Å^3.

For **3**·$3CH_2Cl_2$, a systematic search of a limited hemisphere of reciprocal space located a set of data with no symmetry or systematic absences, indicating a triclinic space group. Subsequent successful solution and refinement of the structure confirmed the choice of the centrosymmetric space group $P\bar{1}$. Following complete data collection and processing, a unique set of 7405 intensities was obtained and gave a residual of 0.137 for reflections measured more than once; 3678 reflections had $F > 4.0\sigma(F)$. No correction was made for absorption. All non-hydrogen atoms were readily located and refined on F^2 with anisotropic thermal parameters; H atoms were included in fixed positions and refined with the use of a riding model in the final least-squares cycles. A final difference Fourier map was essentially featureless, with the largest peak having an intensity of 1.04 e/Å^3 and residing near a manganese atom.

Final values of discrepancy indices for both complexes are included in Table 1.

Physical Measurements. Infrared spectra (KBr disks) were recorded on a Nicolet model 510P spectrophotometer. Variable-temperature, direct current (dc) magnetic susceptibility data were collected using a Quantum Design MPMS SQUID susceptometer in the temperature range 2.00−320 K and in an applied magnetic field of

(12) Libby, E.; McCusker, J. K.; Schmitt, E. A.; Folting, K.; Hendrickson, D. N.; Christou, G. *Inorg. Chem.* **1991**, *30*, 3486.
(13) Hendrickson, D. N.; Christou, G.; Schmitt, E. A.; Libby, E.; Baskin, J. S.; Wang, S.; Tsai, H.-L.; Vincent, J. B.; Boyd, P. D. W.; Huffman, J. C.; Folting, K.; Li, Q.; Streib, W. E. *J. Am. Chem. Soc.* **1992**, *114*, 2455.
(14) Vincent, J. B.; Chang, H.-R.; Folting, K.; Huffman, J. C.; Christou, G.; Hendrickson, D. N. *J. Am. Chem. Soc.* **1987**, *109*, 5703.
(15) Chisholm, M. H.; Folting, K.; Huffman, J. C.; Kirkpatrick, C. C. *Inorg. Chem.* **984**, *23*, 1021.

Table 1. Crystallographic Data for Complexes **2**·6CH_2Cl_2 and **3**·3CH_2Cl_2[a]

	2	**3**
formula[b]	$C_{96}H_{74}N_8O_{36}Cl_{12}Mn_{10}$	$C_{111}H_{82}N_6O_{36}Cl_6Mn_{10}$
fw, g/mol	2890.5	2838.0
space group	$P2_1/n$	$P\bar{1}$
a, Å	14.987(3)	14.892(6)
b, Å	17.177(3)	15.537(6)
c, Å	21.250(4)	14.697(6)
α, deg	90	109.82(2)
β, deg	91.48(1)	97.75(2)
γ, deg	90	111.66(2)
V, Å^3	5469	2839
Z	2	1
T, °C	−169	−165
ρ_{calc}, g/cm^3	1.755	1.660
μ, cm^{-1}	14.484	12.548
R (R_w or $_w$R2), %	5.81 (5.50)[c,d]	8.83 (16.53)[c,e]

[a] Radiation = 0.710 69 Å; graphite monochromator. [b] Including solvate molecules. [c] $R = 100\sum||F_o| - |F_c||/\sum|F_o|$. [d] $R_w = 100[\sum w(|F_o| - |F_c|)^2/\sum w|F_o|^2]^{1/2}$, where $w = 1/\sigma^2(|F_o|)$. [e] $_w$R2 $= 100[\sum w(F_o^2 - F_c^2)^2/\sum w(F_o^2)^2]^{1/2}$.

10 kG. Alternating current (ac) magnetic susceptibility measurements were made on a Quantum Design IT MPMS2 ac SQUID susceptometer operating with a 1 G ac field at a frequency of 250 Hz. The diamagnetic correction was estimated from Pascal's constants and was subtracted from the experimental susceptibility to give the molar paramagnetic susceptibility (χ_m).

Results

Syntheses. It has been previously demonstrated that the reaction of the butterfly anion of $(NBu^n_4)[Mn_4O_2(O_2CR)_7(pic)_2]$ (pic^- = picolinate) with 1 equiv of Me_3SiCl in MeCN solution leads to a site-specific abstraction of one RCO_2^- group to give the $[Mn_4O_2(O_2CR)_6(pic)_2]$ fragment, which dimerizes when R = Me to $[Mn_8O_4(O_2CMe)_{12}(pic)_4]$ or forms $[Mn_4O_2(O_2CPh)_6(MeCN)_2(pic)_2]$ (**1**) when R = Ph.[3c] The present results arise from an investigation of the stability of **1** in mixed solvent systems involving the good donor solvent *N*,*N*-dimethylacetamide (DMA). It was observed that from such solutions slowly crystallize large, well-formed cube-shaped black crystals of a material identified by crystallography as $[Mn_{10}O_8(O_2CPh)_6(pic)_8]$ (**2**), which does not redissolve in any identified organic solvent. The yield was low, typically 15% based on Mn, but consideration of the Mn:pic ratios in **1** *vs* **2** suggests that pic^- is likely the yield-limiting reagent (eq 1), and the yield is 24%

$$8[Mn_4O_2(O_2CR)_6(MeCN)_2(pic)_2] \rightarrow 2[Mn_{10}O_8(O_2CR)_6(pic)_8] + 12Mn^{3+} + ... \quad (1)$$

based on pic^-. The reaction is likely triggered by the good donor properties of DMA which may cause partial or complete displacement of one or more RCO_2^- groups, destabilizing the molecule and initiating the structural transformation; note that no redox change has occurred between **1** ($4Mn^{III}$) and **2** ($10Mn^{III}$). The transformation is undoubtedly complicated, with several species likely present in equilibrium in solution, and the clean formation of a single product can be assigned to the high insolubility of the product, even in DMA, and its consequent crystallization from solution. Note that the remarkable conversion of **1** to **2** requires DMA; it does not occur in neat CH_2Cl_2 or MeCN. Use of DMF instead of DMA also proved unsuccessful, owing to rapid precipitation of $[Mn_4O_2(O_2CPh)_6(DMF)_2(pic)_2]$, as indicated by IR spectral comparison with **1**. Similarly, **2** is not formed if $(NBu^n_4)[Mn_4O_2(O_2CPh)_7(pic)_2]$ is used instead of **1**, supporting the importance of the labile MeCN groups on **1** which undoubtedly provide the initial binding site for DMA molecules.

The considerations summarized in eq 1 suggested that addition of free picH to the reaction solution might increase the yield of **2**; this did indeed turn out to be the case, and a yield of 50−55% was now obtained based on eq 2, which

$$5[Mn_4O_2(O_2CPh)_6(MeCN)_2(pic)_2] + 6picH + 6H_2O \rightarrow 2[Mn_{10}O_8(O_2CPh)_6(pic)_8] + 18PhCO_2H + 10MeCN \quad (2)$$

assumes that solvent and/or atmospheric moisture provide the additional oxide groups required. Further increases in the picH:**1** ratio gave progressively increasing contamination by $[Mn_2O_2(pic)_4]$,[16] shown by IR spectral examination of obtained solids. The ligand dbm^- (where Hdbm is dibenzoylmethane) has in the past led to Mn complexes with favorable solubility properties.[17] Since added picH gave an increased yield of **2**, the same reaction but with added dibenzoylmethane was explored and was found to give the same $[Mn_{10}O_8]^{14+}$ core but with a mixed-chelate environment, the product being $[Mn_{10}O_8(O_2CPh)_6(pic)_6(dbm)_2]$ (**3**). The sample showed no evidence of pic^-/dbm^- disorder, but also was essentially insoluble in all organic solvents, unfortunately.

Initial attempts to prepare the $MeCO_2^-$ version of **2** were foiled by the poor solubility of $[Mn_4O_2(O_2CMe)_6(pic)_2]_2$ in DMA; this neutral complex is the closest to **1** that is available, since $[Mn_4O_2(O_2CMe)_6(MeCN)_2(pic)_2]$ is not known. An alternative route to the desired $[Mn_{10}O_8(O_2CMe)_6(pic)_8]$ (**4**) was instead developed involving the reaction of pic^- with the $3Mn^{III},Mn^{IV}$ complex $[Mn_4O_3Cl_4(O_2CMe)_3(py)_3]$ in CH_2Cl_2, which gives ∼20% isolated yield of **4** based on Mn (method A). A superior method subsequently developed involved the reaction of the neutral $Mn^{II},2Mn^{III}$ complex $[Mn_3O(O_2CMe)_6(py)_3](py)$ in MeCN with picH, followed by oxidation with MnO_4^- to give **4** in 58% isolated yield. Elemental analysis, solubility characteristics, and IR spectral data clearly indicate these products to be the $MeCO_2^-$ analogue of **2**, i.e., $[Mn_{10}O_8(O_2CMe)_6(pic)_8]$ (**4**), and a structural characterization was therefore not pursued.

Description of Structures. ORTEP representations at the 50% probability level of complexes **2** and **3** are shown in Figures 1−3 together with a stereoview of **2** and a representation of its $[Mn_{10}O_8]^{14+}$ core. Fractional coordinates and selected bond distances and angles are collected in Tables 2−5.

For **2**, the structure consists of a $[Mn_{10}(\mu_3\text{-}O)_6(\mu_4\text{-}O)_2]^{14+}$ core lying on an inversion center and containing trigonal pyramidal (μ_3) or distorted tetrahedral (μ_4) bridging O atoms; the former are almost trigonal planar, the sum of angles being in the range 346−349°. Peripheral ligation is provided by eight chelating pic^- and six bridging $PhCO_2^-$ groups; the latter are *all* in fairly rare μ_3 modes,[3b,18] one O bridging two Mn atoms and the other O terminal to a third Mn atom, with the bridging carboxylate O atoms being O(10), O(21), and O(30′). Mn(3)−O(30′) is exceptionally long at 2.597(5) Å. All Mn have distorted octahedral geometry and show the Jahn−Teller (JT) distortion

(16) (a) Hoof, D. L.; Tisley, D. G.; Walton, R. A. *Inorg. Nucl. Chem. Lett.* **1973**, *9*, 571. (b) Matsushita, T.; Spencer, L.; Sawyer, D. T. *Inorg. Chem.* **1988**, *27*, 1167. (c) Libby, E.; Webb, R. J.; Streib, W. E.; Folting, K.; Huffman, J. C.; Hendrickson, D. N.; Christou, G. *Inorg. Chem.* **1989**, *28*, 4037.

(17) Wang, S.; Folting, K.; Streib, W. E.; Schmitt, E. A.; McCusker, J. K.; Hendrickson, D. N.; Christou, G. *Angew. Chem., Int. Ed. Engl.* **1991**, *30*, 305.

(18) (a) Wang, S.; Tsai, H.-L.; Hagen, K. S.; Hendrickson, D. N.; Christou, G. *J. Am. Chem. Soc.* **1994**, *116*, 8376. (b) Schake, A. R.; Vincent, J. B.; Li, Q.; Boyd, P. D. W.; Folting, K.; Huffman, J. C.; Hendrickson, D. N.; Christou, G. *Inorg. Chem.* **1989**, *28*, 1915.

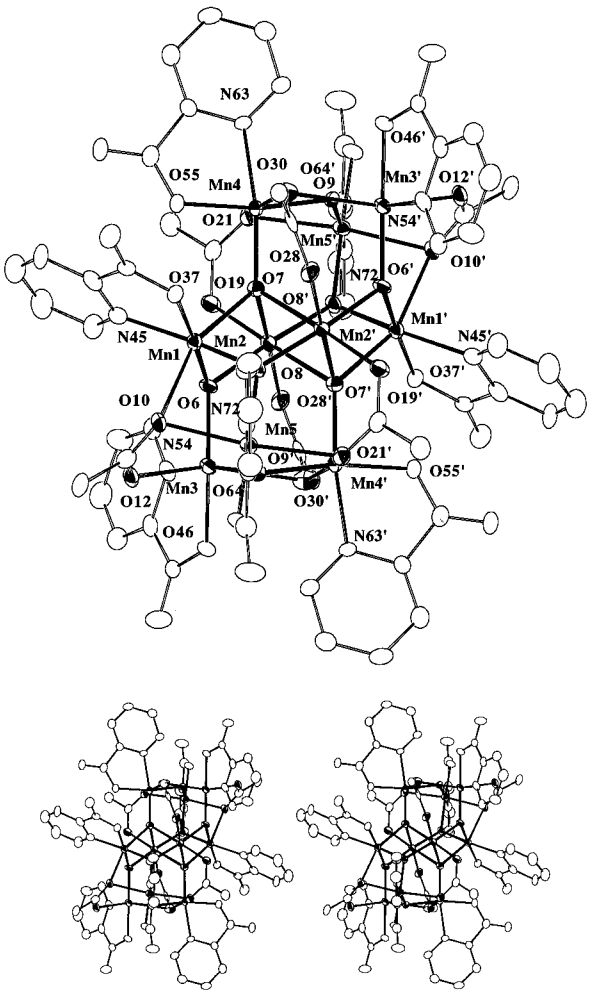

Figure 1. ORTEP representation and stereopair of complex **2**; for clarity, only the *ipso* C atom of phenyl rings is included, and peripheral atoms are de-emphasized. Primed and unprimed atoms are related by the inversion center.

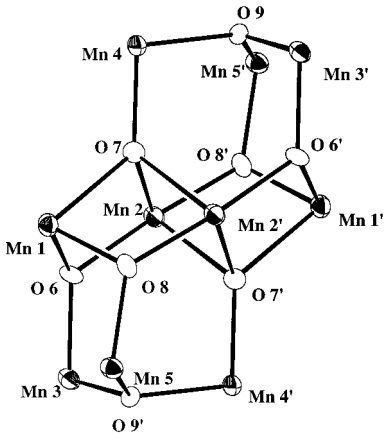

Figure 2. The $[Mn_{10}O_8]^{14+}$ core of complex **2** from a viewpoint the same as that in Figure 1, emphasizing the fused-butterfly structure.

(axial elongation) expected for high-spin Mn^{III} (d^4) ions in this geometry: as is usually the case, the JT axes avoid the short, strong $Mn^{III}-O^{2-}$ bonds, except where this is not possible, i.e., three O^{2-} ions in a *fac* disposition about a Mn atom. Thus, two of the four bonds to O(7) are JT lengthened, Mn(1)−O(7) = 2.171(4) and Mn(2′)−O(7) = 2.317(4) Å, the latter abnormally so: a $Mn^{III}-O^{2-}$ bond greater than 2.3 Å is extremely rare (*vide infra*). In fact, a search of the Cambridge Crystallographic Database revealed no previous examples of such a linkage. As a result of the JT elongated $Mn-O^{2-}$ bonds, even

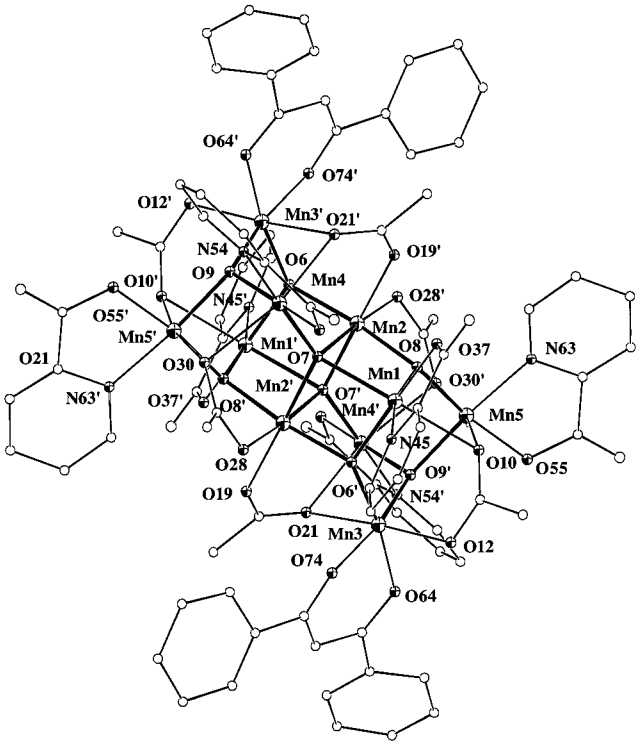

Figure 3. ORTEP representation of complex **3**, with atoms shown as isotropic spheres, from a viewpoint emphasizing the location of the dbm^- groups.

the Mn···Mn separations bridged by *two* O^{2-} ions are long, with all Mn···Mn separations being ∼3.0 Å or greater.

For **3**, the molecule also lies on an inversion center and is essentially isostructural with **2** except that two pic^- groups are replaced by dbm^- groups. The JT elongation axes are in equivalent positions in **2** and **3**. The replacement of pic^- (five-membered chelate ring) with dbm^- (six-membered ring) causes only very minor perturbations; as is emphasized by the view in Figure 3, the dbm^- groups are on Mn(3) and Mn(3′), resulting in very small differences at these positions between **2** and **3**. Synthetic attempts to produce a $[Mn_{10}O_8]^{14+}$ core with dbm^- ligands replacing all pic^- ligands were unsuccessful, possibly because of steric crowding of the additional phenyl rings.

The Mn_{10} topology in **2** and **3** can be described in a number of ways, but the following two are particularly useful. As is emphasized in Figure 2, the $[Mn_{10}O_8]^{14+}$ core can be described as two Mn_3 triangular units above and below a central Mn_4 planar unit, separated by two layers of O^{2-} ions. The central Mn_4 layer can itself be described as two edge-sharing Mn_3 triangular units, and the central $[Mn_4O_6]$ unit as two face-sharing partial-cubane units. A second way of describing the core emphasizes its $[Mn_4O_2]^{8+}$ parentage (i.e., **1**) and incorporates the unusually long, JT elongated $Mn-O^{2-}$ bonds Mn(2)−O(7′) and Mn(2′)−O(7) (2.317(4) Å): it contains two $[Mn_4O_2]^{8+}$ units linked together by these two JT elongated $Mn-O^{2-}$ bonds, as shown in Figure 4. This $[Mn_8O_4]^{16+}$ unit is essentially identical to that in $[Mn_8O_4(O_2CPh)_{12}(Et_2mal)_2(H_2O)_2]^{2-}$ (Et_2mal = 2,2-diethylmalonate) except that the latter has a $[Mn_8O_4]^{14+}$ core, i.e., $2Mn^{II},8Mn^{III}$, with the Mn^{II} ions being at positions Mn(4)/Mn(4′) in Figure 4.[3e] The JT elongated $Mn^{III}-O^{2-}$ bonds (2.258(10) Å) are also abnormally long but slightly shorter than those in **2** (and **3**). In **2** and **3**, additional Mn^{III} and O^{2-} ions then complete the $[Mn_{10}O_8]^{14+}$ core.

Complexes **2** and **3** join only a handful of other Mn_{10} clusters currently known, the others being $[Mn_{10}O_{14}(tren)_6]^{8+}$ ($4Mn^{III}$,-$6Mn^{14}$),[5a] $[Mn_{10}O_2Cl_8((OCH_2)_3CMe)_6]^{2-}$ ($2Mn^{II},8Mn^{III}$),[5d]

Table 2. Selected Fractional Coordinates ($\times 10^4$) and Equivalent Isotropic Thermal Parameters (Å^2, $\times 10$)[a] for $[Mn_{10}O_8(O_2CPh)_6(pic)_8]$ (**2**)

atom	*x*	*y*	*z*	B_{eq}
Mn(1)	165(1)	6510(1)	4847.5(5)	13
Mn(2)	−76(1)	4929(1)	4276.3(5)	12
Mn(3)	−1811(1)	6091(1)	4146.0(5)	13
Mn(4)	2050(1)	5155(1)	4761.3(5)	12
Mn(5)	−1501(1)	6483(1)	5682.8(5)	13
O(6)	−576(3)	5956(2)	4234(2)	14
O(7)	820(3)	5383(2)	4815(2)	12
O(8)	−357(3)	6088(2)	5579(2)	14
O(9)	2002(3)	4091(2)	5001(2)	12
O(10)	−957(3)	7402(2)	5033(2)	15
C(11)	−1456(4)	7700(4)	4609(3)	17
O(12)	−1770(3)	7338(2)	4141(2)	18
C(13)	−1731(5)	8539(4)	4681(3)	20
O(19)	627(3)	5127(3)	3398(2)	17
C(20)	1437(4)	4936(4)	3350(3)	14
O(21)	1891(3)	4592(3)	3787(2)	16
C(22)	1914(5)	5135(4)	2766(3)	20
O(28)	−1016(3)	4476(3)	3714(2)	19
C(29)	1840(4)	5643(4)	6203(3)	16
O(30)	2272(3)	5361(3)	5763(2)	20
C(31)	2335(4)	6114(4)	6689(3)	15
O(37)	982(3)	7080(2)	5382(2)	15
C(38)	1489(4)	7605(4)	5121(3)	17
O(39)	2038(3)	7993(3)	5409(2)	25
C(40)	1348(4)	7677(4)	4427(3)	18
N(45)	730(3)	7186(3)	4175(3)	16
O(46)	−3075(3)	6194(3)	3977(2)	19
C(47)	−3327(4)	6376(4)	3409(3)	20
O(48)	−4073(3)	6616(4)	3261(2)	36
C(49)	−2633(4)	6284(4)	2924(3)	18
N(54)	−1827(4)	6055(3)	3167(2)	16
O(55)	2312(3)	6174(3)	4448(2)	18
C(56)	3090(4)	6321(4)	4221(3)	20
O(57)	3310(3)	6927(3)	3980(2)	26
C(58)	3735(4)	5646(4)	4282(3)	14
N(63)	3375(3)	5022(3)	4573(2)	13
O(64)	−2623(3)	6972(3)	5872(2)	15
C(65)	−2705(4)	7255(4)	6431(3)	19
O(66)	−3398(3)	7461(3)	6662(2)	28
C(67)	−1818(4)	7339(4)	6791(3)	18
N(72)	−1126(4)	7038(3)	6483(2)	15

[a] $B_{eq} = (4/3)\sum\sum B_{ij}a_ia_j$.

Table 3. Selected Fractional Coordinates ($\times 10^4$) and Equivalent Isotropic Thermal Parameters (Å^2, $\times 10^3$)[a] for $[Mn_{10}O_8(O_2CPh)_6(pic)_6(dbm)_2]$ (**3**)

atom	*x*	*y*	*z*	U_{eq}
Mn(1)	4446(1)	5785(2)	3857(2)	25
Mn(2)	4474(1)	5478(1)	5736(2)	24
Mn(3)	2233(1)	4242(2)	3989(2)	27
Mn(4)	6757(1)	7216(1)	5982(2)	26
Mn(5)	3425(1)	3509(2)	2313(1)	28
O(6)	3559(6)	5308(6)	4568(6)	27
O(7)	5510(5)	6056(6)	5192(6)	22
O(8)	4620(5)	4583(6)	3279(6)	21
O(9)	7313(5)	6650(6)	6718(6)	20
O(10)	3134(6)	4804(6)	2319(6)	26
C(11)	2393(11)	4974(10)	2354(10)	28
O(12)	1773(6)	4689(6)	2837(7)	34
C(13)	2113(11)	5503(11)	1721(11)	40
O(19)	3414(6)	4882(6)	6322(6)	26
C(20)	2768(10)	3951(10)	5983(10)	30
O(21)	2500(6)	3314(6)	5081(6)	26
C(22)	2314(9)	3659(10)	6740(10)	29
O(28)	4551(6)	6967(6)	6657(6)	28
C(29)	5407(10)	7724(9)	7194(9)	21
O(30)	6218(6)	7647(6)	7361(6)	25
C(31)	5452(10)	8759(10)	7523(11)	36
O(37)	5331(6)	6448(6)	3206(6)	27
C(38)	5329(10)	7294(10)	3222(10)	30
O(39)	5883(7)	7801(6)	2841(7)	45
C(40)	4670(10)	7647(10)	3752(10)	28
N(45)	4131(7)	6950(8)	4116(7)	25
O(46)	6368(6)	8014(6)	5432(7)	36
C(47)	6984(10)	9007(11)	5713(11)	35
O(48)	6818(7)	9568(7)	5406(7)	44
C(49)	7929(9)	9305(10)	6518(10)	30
N(54)	8011(8)	8589(8)	6762(8)	28
O(55)	2275(6)	2465(6)	1157(6)	27
C(56)	2413(10)	2230(10)	254(11)	37
O(57)	1748(7)	1584(7)	−534(7)	47
C(58)	3439(10)	2885(10)	236(10)	36
N(63)	4069(8)	3559(8)	1188(8)	32
O(64)	874(6)	3138(6)	3593(6)	26
C(65)	348(9)	3072(10)	4176(10)	31
C(72)	499(10)	3866(10)	5096(11)	37
C(73)	1232(11)	4849(11)	5414(11)	39
O(74)	1856(6)	5112(7)	4946(7)	40

[a] U_{eq} = one-third of the trace of the orthogonalized U_{ij} tensor

$[Mn_{10}O_4X_{12}(biphen)_4]^{4-}$ ($6Mn^{II}$,$4Mn^{III}$; X = Cl^-, Br^-),[5b,c] and $[Mn_{10}O_4(OH)_2(O_2CMe)_8(hmp)_8]^{4+}$ [5f] ($10Mn^{III}$; hmpH = 2-(hydroxymethyl)pyridine). None of them has a core similar to those of **2** and **3**.

Magnetochemistry of Complex 2. Solid-state, magnetic susceptibility studies were carried out on complex **2**·$3H_2O$. The bulk sample from which the analytical sample had been taken was stored and handled in an inert-atmosphere glovebox to avoid changes in composition owing to its hygroscopic nature. Variable-temperature dc susceptibility data were collected on powdered samples of this material restrained in parafilm in the 2.00−320 K temperature range and a 10 kG applied magnetic field. The effective magnetic moment (μ_{eff}) per Mn_{10} molecule slowly decreases from 14.28 μ_B at 320 K to 4.94 μ_B at 2.00 K; these correspond to χ_mT values of 25.50 and 3.05 cm^3 K mol^{-1} at 320 and 2.00 K, respectively, and the data are plotted as χ_mT *vs* *T* in Figure 5. The spin-only (g = 2) μ_{eff}/χ_mT values for ten noninteracting Mn^{III} ions are 15.49 μ_B/30.00 cm^3 K mol^{-1}, and Figure 5 thus indicates that there are appreciable antiferromagnetic exchange interactions within complex **2**.

With ten Mn^{III} ions in **2**, the total degeneracy (i.e., order of the spin Hamiltonian matrix) is 5^{10} and total spin (S_T) values are in the 0−20 range. The large number of spin states makes it an extremely difficult task to evaluate the magnetic exchange parameters (J in $\hat{H} = -2J_{ij}\hat{S}_i\hat{S}_j$) that characterize the pairwise magnetic exchange interactions in the complex; a matrix diagonalization approach would involve diagonalizing a matrix of approximate dimensions 9.8×10^6 by 9.8×10^6. Unfortunately, the number of metal ions and the topology of the Mn_{10} complex also rule out an equivalent operator approach based on the Kambe vector coupling method.[19]

The χ_mT *vs* *T* data for complex **2** in Figure 5 appear to be heading for 0 at 0 K and suggest an $S_T = 0$ ground state. An expansion of the 2.00−30.0 K data region is shown in Figure 6, together with the ac magnetic susceptibility data measured in this temperature range on a Quantum Design SQUID susceptometer. The ac data were measured in 0 dc field with a 1.0 G ac field oscillating at 1000 Hz. The ac and dc data are essentially superimposable except at the lowest temperatures, probably due to saturation of the magnetization in the 10.0 kG field. Although data at <2.00 K would be required to confirm this, the plots of Figure 6 are consistent with an $S_T = 0$ ground state for the complex, with very low-lying excited states that are populated even at 2.00 K. However, the possibility of an $S_T = 1$ (or even $S_T = 2$) ground state with low-lying excited states cannot be ruled out with certainty. Clearly, the spin of the ground state of the complex is small. It should also be noted

(19) Kambe, K. *J. Phys. Soc. Jpn.* **1950**, *48*, 15.

Table 4. Selected Interatomic Distances (Å) and Angles (deg) for $[Mn_{10}O_8(O_2CPh)_6(pic)_8]$ (**2**)

Mn(1)−Mn(2)	2.992(2)	Mn(2)−Mn(4)	3.346(2)
Mn(1)−Mn(2′)	3.099(2)	Mn(2)−Mn(4′)	3.642(2)
Mn(1)−Mn(3)	3.359(2)	Mn(2)−Mn(5′)	3.386(2)
Mn(1)−Mn(4)	3.668(2)	Mn(3)−Mn(4′)	3.186(2)
Mn(1)−Mn(5)	3.100(2)	Mn(3)−Mn(5)	3.355(2)
Mn(2)−Mn(2′)	3.088(2)	Mn(4)−Mn(5′)	3.074(2)
Mn(2)−Mn(3)	3.284(2)		
Mn(1)−O(6)	1.940(4)	Mn(3)−O(30′)	2.597(5)
Mn(1)−O(7)	2.171(4)	Mn(3)−O(46)	1.926(4)
Mn(1)−O(8)	1.901(4)	Mn(3)−N(54)	2.081(5)
Mn(1)−O(10)	2.317(4)	Mn(4)−O(7)	1.890(4)
Mn(1)−O(37)	1.917(4)	Mn(4)−O(9)	1.900(4)
Mn(1)−N(45)	2.042(6)	Mn(4)−O(21)	2.292(4)
Mn(2)−O(6)	1.918(4)	Mn(4)−O(30)	2.175(5)
Mn(2)−O(7)	1.910(4)	Mn(4)−O(55)	1.917(4)
Mn(2)−O(7′)	2.317(4)	Mn(4)−N(63)	2.049(5)
Mn(2)−O(8′)	1.887(4)	Mn(5)−O(8)	1.862(4)
Mn(2)−O(19)	2.194(4)	Mn(5)−O(9′)	1.894(4)
Mn(2)−O(28)	1.982(4)	Mn(5)−O(10)	2.262(4)
Mn(3)−O(6)	1.869(4)	Mn(5)−O(21′)	2.249(4)
Mn(3)−O(9′)	1.870(4)	Mn(5)−O(64)	1.932(4)
Mn(3)−O(12)	2.142(4)	Mn(5)−N(72)	2.017(5)

O(6)−Mn(1)−O(7)	78.13(16)	O(7)−Mn(4)−O(21)	93.65(17)
O(6)−Mn(1)−O(8)	97.02(18)	O(7)−Mn(4)−O(30)	91.81(17)
O(6)−Mn(1)−O(10)	91.87(16)	O(7)−Mn(4)−O(55)	92.32(18)
O(6)−Mn(1)−O(37)	173.85(18)	O(7)−Mn(4)−N(63)	170.56(20)
O(6)−Mn(1)−N(45)	92.79(20)	O(9)−Mn(4)−O(21)	80.32(17)
O(7)−Mn(1)−O(8)	83.25(17)	O(9)−Mn(4)−O(30)	84.27(18)
O(7)−Mn(1)−O(10)	157.76(16)	O(9)−Mn(4)−O(55)	168.90(18)
O(7)−Mn(1)−O(37)	101.01(17)	O(9)−Mn(4)−N(63)	89.30(19)
O(7)−Mn(1)−N(45)	106.78(19)	O(21)−Mn(4)−O(30)	164.23(17)
O(8)−Mn(1)−O(10)	78.28(16)	O(21)−Mn(4)−O(55)	95.09(18)
O(8)−Mn(1)−O(37)	88.90(18)	O(21)−Mn(4)−N(63)	81.68(18)
O(8)−Mn(1)−N(45)	167.28(20)	O(30)−Mn(4)−O(55)	99.47(19)
O(10)−Mn(1)−O(37)	90.97(17)	O(30)−Mn(4)−N(63)	94.85(19)
O(10)−Mn(1)−N(45)	93.37(18)	O(55)−Mn(4)−N(63)	80.00(20)
O(37)−Mn(1)−N(45)	81.60(20)	O(8)−Mn(5)−O(9′)	93.86(18)
O(6)−Mn(2)−O(7′)	93.23(17)	O(8)−Mn(5)−O(10)	80.48(17)
O(6)−Mn(2)−O(7)	85.44(18)	O(8)-Mn(5)−O(21′)	90.69(17)
O(6)−Mn(2)−O(8′)	172.73(19)	O(8)−Mn(5)−O(64)	172.95(19)
O(6)−Mn(2)−O(19)	90.75(17)	O(8)−Mn(5)−N(72)	92.03(20)
O(6)−Mn(2)−O(28)	93.58(18)	O(9′)−Mn(5)−O(10)	92.11(17)
O(7)−Mn(2)−O(7′)	86.64(17)	O(9′)−Mn(5)−O(21′)	81.58(17)
O(7′)−Mn(2)−O(8′)	79.64(17)	O(9′)−Mn(5)−O(64)	93.18(18)
O(7)−Mn(2)−O(8′)	92.67(18)	O(9′)−Mn(5)−N(72)	171.36(20)
O(7′)−Mn(2)−O(19)	175.48(16)	O(10)−Mn(5)−O(21′)	168.82(16)
O(7)−Mn(2)−O(19)	95.82(17)	O(10)−Mn(5)−O(64)	98.83(17)
O(7′)−Mn(2)−O(28)	93.50(17)	O(10)−Mn(5)−N(72)	95.08(19)
O(7)−Mn(2)−O(28)	179.02(19)	O(21′)−Mn(5)−O(64)	90.76(17)
O(8′)−Mn(2)−O(19)	96.43(18)	O(21′)−Mn(5)−N(72)	92.05(19)
O(8′)−Mn(2)−O(28)	88.31(19)	O(64)−Mn(5)−N(72)	81.02(20)
O(19)−Mn(2)−O(28)	84.11(18)	Mn(1)−O(6)−Mn(2)	101.69(19)
O(6)−Mn(3)−O(9′)	93.33(18)	Mn(1)−O(6)−Mn(3)	123.70(22)
O(6)−Mn(3)−O(12)	95.52(18)	Mn(2)−O(6)−Mn(3)	120.23(22)
O(6)−Mn(3)−O(30′)	97.93(17)	Mn(1)−O(7)−Mn(2)	94.07(17)
O(6)−Mn(3)−O(46)	174.68(20)	Mn(1)−O(7)−Mn(2′)	87.28(14)
O(6)−Mn(3)−N(54)	94.69(20)	Mn(1)−O(7)−Mn(4)	128.98(21)
O(9′)−Mn(3)−O(12)	100.18(18)	Mn(2)−O(7)−Mn(2′)	93.36(17)
O(9′)−Mn(3)−O(30′)	73.71(16)	Mn(2)−O(7)−Mn(4)	123.40(22)
O(9′)−Mn(3)−O(46)	91.26(19)	Mn(2′)−O(7)−Mn(4)	119.58(20)
O(9′)−Mn(3)−N(54)	165.17(20)	Mn(1)−O(8)−Mn(2′)	109.83(21)
O(12′)−Mn(3)−O(30′)	165.51(16)	Mn(1)−O(8)−Mn(5)	110.98(21)
O(12)−Mn(3)−O(46)	86.29(18)	Mn(2′)−O(8)−Mn(5)	129.20(23)
O(12)−Mn(3)−N(54)	91.45(20)	Mn(3′)−O(9)−Mn(4)	115.36(21)
O(30′)−Mn(3)−O(46)	80.79(17)	Mn(3)−O(9)−Mn(5′)	126.09(22)
O(30′)−Mn(3)−N(54)	92.81(19)	Mn(4)−O(9)−Mn(5′)	108.22(21)
O(46)−Mn(3)−N(54)	80.25(20)	Mn(1)−O(10)−Mn(5)	85.23(14)
O(7)−Mn(4)−O(9)	98.03(18)	Mn(4)−O(21)−Mn(5′)	85.21(15)

that no out-of-phase signal was observed in the ac susceptibility studies in the 2.00−30.0 K range with a 1 G ac field oscillating at 250 Hz.

The results on complex **2** may be compared with those obtained on other high nuclearity Mn_x ($x \geq 8$) carboxylate clusters:[20] with the exception of $[Mn_{18}K_4O_{16}(O_2CPh)_{22}(phth)_2(H_2O)_4]$ ($phth^{2-}$ = phthalate),[10] which has an $S_T = 0$, all other related clusters have $S_T \geq 3$; for example, $[Mn_8O_4(O_2CPh)_{12}(Et_2mal)_2(H_2O)_2]^{2-}$ (Et_2mal = 2,2-diethylmalonate),[3e] $[Mn_8O_6Cl_6(O_2CPh)_7(H_2O)_2]^-$,[3b] and $[Mn_9Na_2O_7(O_2CPh)_{15}(MeCN)_2]$[3b] have $S_T = 3$, 11, and 4, respectively. $[Mn_{10}O_4X_{12}$-

Table 5. Selected Interatomic Distances (Å) and Angles (deg) for $[Mn_{10}O_8(O_2CPh)_6(pic)_6(dbm)_2]$ (**3**)

Mn(1)−Mn(2)	2.956(3)	Mn(2)−Mn(4)	3.348(3)
Mn(1)−Mn(2′)	3.108(3)	Mn(2)−Mn(4′)	3.630(3)
Mn(1)−Mn(3)	3.362(3)	Mn(2)−Mn(5′)	3.372(3)
Mn(1)−Mn(4)	3.645(3)	Mn(3)−Mn(4′)	3.156(3)
Mn(1)−Mn(5)	3.103(3)	Mn(3)−Mn(5)	3.360(3)
Mn(2)−Mn(2′)	3.130(4)	Mn(4)−Mn(5′)	3.081(3)
Mn(2)−Mn(3)	3.322(3)		
Mn(1)−O(6)	1.887(8)	Mn(3)−O(74)	1.898(10)
Mn(1)−O(8)	1.902(8)	Mn(3)−O(64)	1.955(8)
Mn(1)−O(37)	1.929(8)	Mn(3)−O(12)	2.157(9)
Mn(1)−N(45)	1.962(11)	Mn(4)−O(9)	1.888(8)
Mn(1)−O(7)	2.156(8)	Mn(4)−O(7)	1.890(7)
Mn(1)−O(10)	2.351(8)	Mn(4)−O(46)	1.901(9)
Mn(2)−O(8′)	1.894(8)	Mn(4)−N(54)	2.043(10)
Mn(2)−O(7)	1.903(8)	Mn(4)−O(21′)	2.147(9)
Mn(2)−O(6)	1.917(8)	Mn(4)−O(30)	2.262(8)
Mn(2)−O(19)	1.979(8)	Mn(5)−O(8)	1.867(7)
Mn(2)−O(28)	2.198(9)	Mn(5)−O(55)	1.935(8)
Mn(2)−O(7′)	2.322(8)	Mn(5)−O(9′)	1.939(8)
Mn(3)−O(9′)	1.834(8)	Mn(5)−N(63)	2.030(10)
Mn(3)−O(6)	1.882(7)	Mn(5)−O(10)	2.207(9)
Mn(3)−O(21)	2.577(10)	Mn(5)−O(30′)	2.227(9)

O(6)−Mn(1)−O(8)	96.8(4)	O(7)−Mn(4)−O(46)	90.9(4)
O(6)−Mn(1)−O(37)	171.9(4)	O(9)−Mn(4)−N(54)	89.7(4)
O(8)−Mn(1)−O(37)	91.4(4)	O(7)−Mn(4)−N(54)	171.4(4)
O(6)−Mn(1)−N(45)	89.7(4)	O(46)−Mn(4)−N(54)	80.6(4)
O(8)−Mn(1)−N(45)	166.3(4)	O(9)−Mn(4)−O(21′)	84.2(3)
O(37)−Mn(1)−N(45)	82.3(4)	O(7)−Mn(4)−O(21′)	91.2(3)
O(6)−Mn(1)−O(7)	79.3(3)	O(46)−Mn(4)−O(21′)	99.2(4)
O(8)−Mn(1)−O(7)	83.2(3)	N(54)−Mn(4)−O(21′)	91.5(4)
O(37)−Mn(1)−O(7)	101.9(3)	O(9)−Mn(4)−O(30)	80.3(3)
N(45)−Mn(1)−O(7)	109.8(4)	O(7)−Mn(4)−O(30)	93.5(3)
O(6)−Mn(1)−O(10)	91.1(3)	O(46)−Mn(4)−O(30)	95.7(4)
O(8)−Mn(1)−O(10)	76.5(3)	N(54)−Mn(4)−O(30)	86.2(4)
O(37)−Mn(1)−O(10)	90.7(3)	O(21′)−Mn(4)−O(30)	164.3(3)
N(45)−Mn(1)−O(10)	91.5(4)	O(8)−Mn(5)−O(55)	170.9(4)
O(7)−Mn(1)−O(10)	156.4(3)	O(8)−Mn(5)−O(9′)	95.1(3)
O(8′)−Mn(2)−O(7)	92.8(3)	O(55)−Mn(5)−O(9′)	93.5(3)
O(8′)−Mn(2)−O(6)	169.1(4)	O(8)−Mn(5)−N(63)	90.6(4)
O(7)−Mn(2)−O(6)	85.3(3)	O(55)−Mn(5)−N(63)	80.7(4)
O(8′)−Mn(2)−O(19)	86.3(3)	O(9′)−Mn(5)−N(63)	174.2(4)
O(7)−Mn(2)−O(19)	179.1(4)	O(8)−Mn(5)−O(10)	80.9(3)
O(6)−Mn(2)−O(19)	95.6(3)	O(55)−Mn(5)−O(10)	96.1(3)
O(8′)−Mn(2)−O(28)	98.5(3)	O(9′)−Mn(5)−O(10)	91.6(3)
O(7)−Mn(2)−O(28)	93.3(3)	N(63)−Mn(5)−O(10)	89.3(4)
O(6)−Mn(2)−O(28)	92.4(3)	O(8)−Mn(5)−O(30′)	92.0(3)
O(19)−Mn(2)−O(28)	86.7(3)	O(55)−Mn(5)−O(30′)	92.2(3)
O(8′)−Mn(2)−O(7′)	79.0(3)	O(9′)−Mn(5)−O(30′)	80.2(3)
O(7)−Mn(2)−O(7′)	84.9(3)	N(63)−Mn(5)−O(30′)	99.8(4)
O(6)−Mn(2)−O(7′)	90.1(3)	O(10)−Mn(5)−O(30′)	168.6(3)
O(19)−Mn(2)−O(7′)	95.1(3)	Mn(3)−O(6)−Mn(1)	126.2(4)
O(28)−Mn(2)−O(7′)	176.8(3)	Mn(3)−O(6)−Mn(2)	122.0(4)
O(9′)−Mn(3)−O(6)	91.1(3)	Mn(1)−O(6)−Mn(2)	102.0(4)
O(9′)−Mn(3)−O(74)	168.2(4)	Mn(4)−O(7)−Mn(2)	123.9(4)
O(9′)−Mn(3)−O(21)	73.8(4)	Mn(4)−O(7)−Mn(1)	128.4(4)
O(6)−Mn(3)−O(21)	94.6(4)	Mn(2)−O(7)−Mn(1)	93.2(3)
O(12)−Mn(3)−O(21)	167.5(4)	Mn(4)−O(7)−Mn(2′)	118.7(4)
O(21)−Mn(3)−O(64)	78.2(4)	Mn(2)−O(7)−Mn(2′)	95.1(3)
O(21)−Mn(3)−O(74)	94.9(4)	Mn(1)−O(7)−Mn(2′)	87.8(3)
O(6)−Mn(3)−O(74)	86.9(4)	Mn(5)−O(8)−Mn(2′)	127.4(4)
O(9′)−Mn(3)−O(64)	91.6(3)	Mn(5)−O(8)−Mn(1)	110.8(4)
O(6)−Mn(3)−O(64)	171.2(4)	Mn(2′)−O(8)−Mn(1)	109.9(4)
O(74)−Mn(3)−O(64)	88.8(4)	Mn(3′)−O(9)−Mn(4)	115.9(4)
O(9′)−Mn(3)−O(12)	100.0(4)	Mn(3′)−O(9)−Mn(5′)	125.8(4)
O(6)−Mn(3)−O(12)	96.4(4)	Mn(4)−O(9)−Mn(5′)	107.2(4)
O(74)−Mn(3)−O(12)	91.7(4)	Mn(5)−O(10)−Mn(1)	85.7(3)
O(64)−Mn(3)−O(12)	91.3(3)	Mn(3)−O(21)−Mn(4′)	83.3(3)
O(9)−Mn(4)−O(7)	98.8(3)	Mn(5′)−O(30)−Mn(4)	86.7(3)
O(9)−Mn(4)−O(46)	169.7(4)		

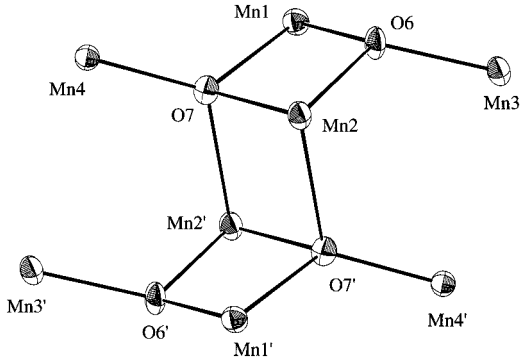

Figure 4. The $[Mn_8O_4]$ fragment within the core of **2** (and **3**) emphasizing the linkage of two $[Mn_4O_2]$ units by two JT elongated $Mn^{III}-O^{2-}$ bonds.

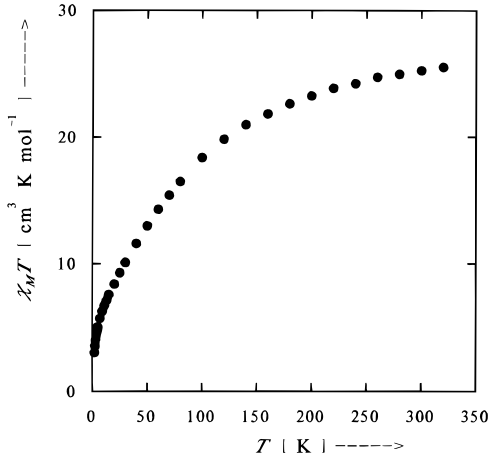

Figure 5. Plot of $\chi_m T$ vs T data for $[Mn_{10}O_8(O_2CPh)_6(pic)_8]\cdot 3H_2O$ ($\mathbf{2}\cdot 3H_2O$). χ_m is the molar dc magnetic susceptibility measured in a 10 kG field.

$(biphen)_4]^{4-}$ (X = Cl, Br; biphen = 2,2′-biphenoxide)[5b,c] and $[Mn_6(hfac)_{12}(NITPh)_6]$ (hfac = hexafluoroacetylacetonate; NITPh = nitronyl nitroxide radical)[21] both have $S_T = 12$, the highest yet observed for Mn clusters of any type. The clusters $[Mn_{12}O_{12}(O_2CR)_{16}(H_2O)_4]^z$ have $S_T = 9$ or 10 ($z = 0$) or $S_T = {}^{19}/_2$ ($z = -1$).[8e,22]

Conclusions

The $[Mn_{10}O_8]^{14+}$ core forms readily upon the DMA-induced transformation of the picolinate complex **1**, leading to the new complexes **2** and **3**. These are new members of the growing class of high nuclearity Mn carboxylate clusters and contain an interesting arrangement of 10 Mn^{III} ions that can be approximately described as the linkage of two $[Mn_4O_2]^{8+}$ butterfly units as found in the parent complex **1**. It is a common theme in high nuclearity Mn carboxylate structural chemistry that the $[Mn_xO_y]$ core may be described as the fusion or linkage of $[Mn_4O_2]^{8+}$ units,[20] although this does not necessarily imply anything with regards to their mechanism of assembly.

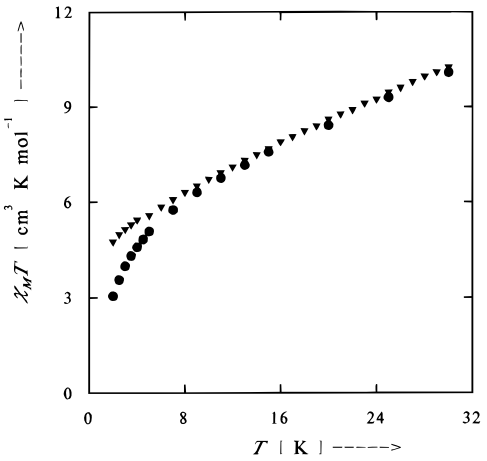

Figure 6. Plot of $\chi_m T$ vs T data for $[Mn_{10}O_8(O_2CPh)_6(pic)_8]\cdot 3H_2O$ ($\mathbf{2}\cdot 3H_2O$) in the 2.00−30.0 K range from ac magnetic susceptibility measurements (▼) and including the dc data (●) from Figure 5 for this temperature range. The ac data were measured in 0 dc field with a 1.0 G ac field oscillating at 1000 Hz.

In contrast to most other high nuclearity Mn_x clusters, complex **2** has a low ground state spin value. It is clear that $[Mn_{10}O_8]^{14+}$-containing complexes are not, unfortunately, new examples of species that (i) possess large spin values in the ground state or (ii) exhibit out-of-phase signals in their ac magnetic susceptibilities characteristic of the slow magnetic relaxation that is taken as evidence of single-molecule magnets.[8e,22,23] New additions to the family of complexes with one or both of the above properties are at hand, however, and will be reported in due course.

Acknowledgment. This work was supported by National Science Foundation Grants CHE-9391104 (G.C.) and CHE-9420322 (D.N.H.). H.J.E. is a National Science Foundation Predoctoral Fellow and the recipient of a Proctor and Gamble Fellowship. We thank Eduardo Libby for experimental assistance with method A for complex **4**. The ac SQUID susceptometer was provided by the Center for Interface and Material Science, funded by the W. A. Keck Foundation.

Supporting Information Available: Textual summaries of the data collection and structure solutions for $\mathbf{2}\cdot 6CH_2Cl_2$ and $\mathbf{3}\cdot 3CH_2Cl_2$, and tables of atomic coordinates, thermal parameters, and bond distances and angles for both structures (34 pages). Ordering information is given on any current masthead page.

IC9607548

(20) Christou, G. In *Magnetism: a Supramolecular Function*; Kahn, O., Ed.; Kluwer Academic: Dordrecht, The Netherlands, 1996; pp 383−409.

(21) Caneschi, A.; Gatteschi, D.; Laugier, J.; Rey, P.; Sessoli, R.; Zanchini, C. *J. Am. Chem. Soc.* **1988**, *110*, 2795.

(22) (a) Sessoli, R.; Tsai, H.-L.; Schake, A. R.; Wang, S.; Vincent, J. B.; Folting, K.; Gatteschi, D.; Christou, G.; Hendrickson, D. N. *J. Am. Chem. Soc.* **1993**, *115*, 1804. (b) Caneschi, A.; Gatteschi, D.; Sessoli, R.; Novak, M. A. *Nature* **1993**, *365*, 141.

(23) Tsai, H.-L.; Eppley, H. J.; de Vries, N.; Folting, K.; Christou, G.; Hendrickson, D. N. *Mol. Cryst. Liq. Cryst.* **1995**, *274*, 167.